Talanta 98 (2012) 7–13

Contents lists available at SciVerse ScienceDirect

Talanta

journal homepage: www.elsevier.com/locate/talanta

Label-free electrochemical aptasensor for sensitive thrombin detection using layer-by-layer self-assembled multilayers with toluidine blue–graphene composites and gold nanoparticles

Shunbi Xie, Ruo Yuan*, Yaqin Chai, Lijuan Bai, Yali Yuan, Yan Wang

Key Laboratory on Luminescence and Real-Time Analysis, Ministry of Education, Key Laboratory of Eco-environments in Three Gorges Reservoir Region, College of Chemistry and Chemical Engineering, Southwest University, Chongqing 400715, PR China

ARTICLE INFO

Article history:
Received 7 March 2012
Received in revised form
6 June 2012
Accepted 9 June 2012
Available online 22 June 2012

Keywords:
Electrochemical aptasensor
Layer-by-layer
Lable-free
Thrombin

ABSTRACT

In the present study, toluidine blue–graphene (Tb–Gra) nanocomposites were prepared to design a Lable-free electrochemical aptasensor for highly sensitive detection of thrombin based on layer-by-layer (LBL) technology. The nanocomposites with excellent redox electrochemical activities were first immobilized on the gold nanoparticles (nano-Au) modified glassy carbon electrodes (GCE). Then, the LBL structure was performed by electrostatic adsorption between the positively charged Tb–Gra and negatively charged nano-Au, which formed $\{Tb–Gra/nano-Au\}_n$ multilayer films for electroactive species enrichment and biomolecule immobilization. Subsequently, the thiolated thrombin binding aptamer (TBA) was assembled on the nano-Au surface through Au–S bond. In the presence of target thrombin (TB), the TBA on the multilayer could catch the thrombin onto the electrode surface, which resulted in a barrier for electro-transfer, leading to the decrease of the electrochemical signal of Tb–Gra nanocomposites. Under the optimal conditions, a wide detection range from 0.001 nM to 80 nM and a low detection limit of 0.33 pM (defined as $S/N=3$) for thrombin were obtained. In addition, the sensor exhibited excellent selectivity against other proteins.

1. Introduction

Aptamers are artificial selected single-stranded DNA/RNA oligonucleotides (40–100 bases) with a unique three dimensional structure, which could provide for binding of their specific target molecules [1]. Aptamers have been an ideal sensing element in the biochemical analysis for their remarkable target diversity, high binding affinity, convenient automated-synthesis, ease-of labeling, and high stability [2–5]. Thrombin is a coagulation protein in the blood stream that has many effects in the coagulation cascade. Excessive TB will induce thrombosis while low content of TB will induce an excessive bleeding [6]. Moreover, it is considered as a useful tumor marker in the diagnosis of pulmonary metastasis [7]. Therefore, sensitive determination of thrombin is very important in clinical research and diagnosis. Up to now, a lot of aptamer-based detection systems for thrombin have been developed such as optical transduction [8], electrochemiluminescence [9], fluorescence [10], colorimetry [11], and electrochemistry [12–14]. Among them, the electrochemical methods have attracted substantial attention in the development of aptasensors because they provided a simple sensitive and selective platform for molecular detection [15].

Graphene, a one-atom-thick planar sheet of sp^2-bonded carbon atoms, is a two-dimension (2D) honeycomb nanostructure, which has attracted rapidly growing research interest since its discovery by Geim in 2004 [16–18]. Significant progress has been made for the utilization of graphene in nanoelectronics and nanocomposites [19] in the recent years by virtue of its outstanding physical, chemical properties and excellent electrocatalytic ability [20–23]. Accordingly, substantial recent research efforts are directed toward the application of graphene-based materials for the design of biosensors, such as Gong and co-works used grahene-based nanomaterials for ultrasensitive detection of cancer biomarker [24], Zhang's group used nanogold-enwrapped graphene nanocomposites as trace lable to quantify carcinoembryonic antigen [25], and Kong et al. explored the nanoparticles–thionine–graphene nanocomposites based immunosensor [26]. The toluidine blue is widely investigated as a feasible redox probe for electrochemical sensors due to its good chemical stability and high electrical conductivity. Therefore, we synthesized the Tb–Gra nanocomposites, which possess the both advantages of grapheme and toluidine blue. The nanocomposites exhibited the following advantages: first of all, the high surface area of graphene is helpful for loading large amount of Tb, which was important for

* Corresponding author. Tel./fax: +86 23 68252277.
E-mail address: yuanruo@swu.edu.cn (R. Yuan).

0039-9140/$ - see front matter © 2012 Elsevier B.V. All rights reserved.
http://dx.doi.org/10.1016/j.talanta.2012.06.019

highly sensitive aptasensor. Meanwhile, the excellent conductivity and small band gap of graphene are favorable for electron transfer between Tb and the electrode; In addition, the nanocomposites provide a good biocompatible microenvironment for the immobilization of aptamer and keep an excellent stability. Due to their good biocompatibility, conductivity and stability [27], gold nanoparticles have been employed to increase the immobilization amount of biological molecules and promote the electronic transfer to magnify current signal [28–29]. Graphene-based materials and gold nanoparticles possessed great potential to fabricate the electrochemical sensor, so we employ graphene and gold nanoparticles as essential parts of the aptasensor.

The LBL self-assembly methods have many advantages compared to conventional coating methods [30], including the simplicity of the LBL process and equipment, its suitability to coating most surfaces, the formation of stabilizing coats and control over the required multilayer thickness [31–34]. Furthermore, compared with monomolecular layers, these LBL multilayers can bring in more probes to produce an amplified signal to improve the sensitivity of the detection. A series of electrochemical sensors have been developed using LBL techniques constructed by combining DNA with redox-active polycations while only few papers have reported the application of aptermer-based on LBL technique [35–36]. Thus, we construct an electrochemical aptasensor based on LBL technique.

In this work, we presented a facile strategy to prepare the self-assembled $\{Tb–Gra/nano-Au\}_n$ multilayer for thrombin detection via an effective LBL technique. To fabricate the nanocomposites, toluidine blue was initially noncovalently bound to the graphene through π–π stacking to form a novel redox hybrid material (Tb–Gra). The thiolated TBA was appended on the modified electrode through Au–S bond. When thrombin is present, it interacts with the TBA strand, forming TB–TBA complex on the electrode interface. The complex is a biological macromolecule, and is not electrochemically active, so will make a barrier for electrons and insulated the conductive support and hindered the transport of electrons toward the electrode surface. This leads to a decrease of current which could be used to detect the target. According to the linearity between TB concentration and current response, we could quantitatively detect target TB. Such sensing strategy provides a new model for importing LBL techniques into the label-free aptamer-based sensing. Meanwhile, other performance characteristics of the sensing system, such as stability and selectivity were also investigated.

2. Experimental section

2.1. Reagents

Thrombins (TB), gold chloride ($HAuCl_4$), toluidine blue, bovine-serum albumin (BSA), hemoglobin (HB), hexanethiol (96%, HT), were obtained from Sigma Chmical Co. (St. Louis, MO, USA). Graphene was purchased from Nanjing Xianfeng Nano Co. (Nanjing, China). Trishydroxymethylaminomethane-hydrochloride (Tris) was purchased from Roche (Switzerland). Thrombin aptamer (TBA): 5′-SH-$(CH_2)_6$-GGT TGG TGT GGT TGG-3′ was purchased from TaKaRa (Dalian, China). All other chemicals were of reagent grade and used as received 0.10 M sodium phosphate buffer (PBS) containing 0.1 M KCl (pH 7.00) was used as working buffer solution. All the TBA samples were dissolved in the 20 mM Tris–HCl buffer (pH 7.4) containing 140 mM NaCl, 5 mM KCl, 1 mM $CaCl_2$ and 1 mM $MgCl_2$. Different concentrations of TB were dissolved in the same Tris–HCl buffer. The nano-Au were prepared according to the literature [37]. Protein solutions were stored at 4 °C before use. Double distilled water was used throughout this study.

2.2. Apparatus

Cyclic voltammetry (CV) was realized through a CHI 660A electrochemical workstation (Shanghai Chenhua Instrument, China). The value of pH was measured by pH meter (MP 230, Mettler-Toledo, Switzerland). The electrochemical system consisted of a three-electrode system where bare or modified glassy carbon electrodes (GCE, Φ=4 mm) were used as a working electrode, platinum wire as an auxiliary electrode and saturated calomel as a reference electrode (SCE). Atomic force microscopy (AFM) was performed on a SPI3800N microscope instrument (Seiko Instruments, Inc., Japan) in tapping-mode in air at ambient temperature.

2.3. The fabrication of the aptasensors

The glassy carbon electrodes were carefully polished with 0.3 and 0.05 alumina powders separately, after rinsing with distilled water the electrodes were ultrasonically rinsed with water and absolute alcohol for 5 min, respectively. And then, they were rinsed with distilled water and dried at room temperature.

First, gold nanoparticles were deposited onto the GCE in 1% $HAuCl_4$ solution at the potential of −0.2 V for 30 s. After dried in the air, 10 μL Tb–Gra nanocomposites were coated on the surface of the electrode for 40 min at room temperature. Following that, the modified electrodes were immersed in nano-Au solution (16 nm) for 20 min to form a nano-Au layer. The $\{Tb–Gra/nano-Au\}_n$ multilayer films were formed by alternately dipping the Tb–Gra nanocomposites on the modified electrode surface for 40 min and immersing in nano-Au solution for 20 min, respectively. Subsequently, 20 μL TBA prepared by the binding buffer was dropped onto the surface of the $\{Tb–Gra/nano-Au\}_n$ multilayer films and incubated for 16 h at 4 °C. Finally, 20 μL hexanethiol solutions (HT, 1 mM) was placed on the surface of the modified electrodes for 40 min to reduce the nonspecific adoption and obtain an optimal nucleic acid orientation. The electrodes were then rinsed with washing buffer and stored at 4 °C prior to electrochemical characterization. The fabrication process of the electrochemical aptasensor is schematically illustrated in Fig. 1.

2.4. Experimental measurements

The electrochemical signal of the modified electrode was investigated by CV with range from −0.6 V to 0.2 V (vs. SCE) at 100 m V s^{-1} in 0.1 M PBS (pH 7.0) containing 0.1 M KCl at room temperature. The fabricated aptasensor was dropped with 20 μL of a fixed concentration of TB for 40 min. The TB detection was based on the changes of the current response ($\Delta I = I_0 - I$). There was a redox peak before the target TB identification, and after the aptasensor combined with TB, the bulky TB molecules perturbed the interfacial electrons transfer which led to a decreased electrochemical signal.

3. Results and discussion

3.1. The electrochemical characterization of the stepwise modified electrodes

To characterize the modified electrode, the assembly steps of the sensing interface were investigated by CV measurements. CVs of different modified electrodes that investigated in PBS solution were shown in Fig. 2. The bare GCE had no obvious redox peak

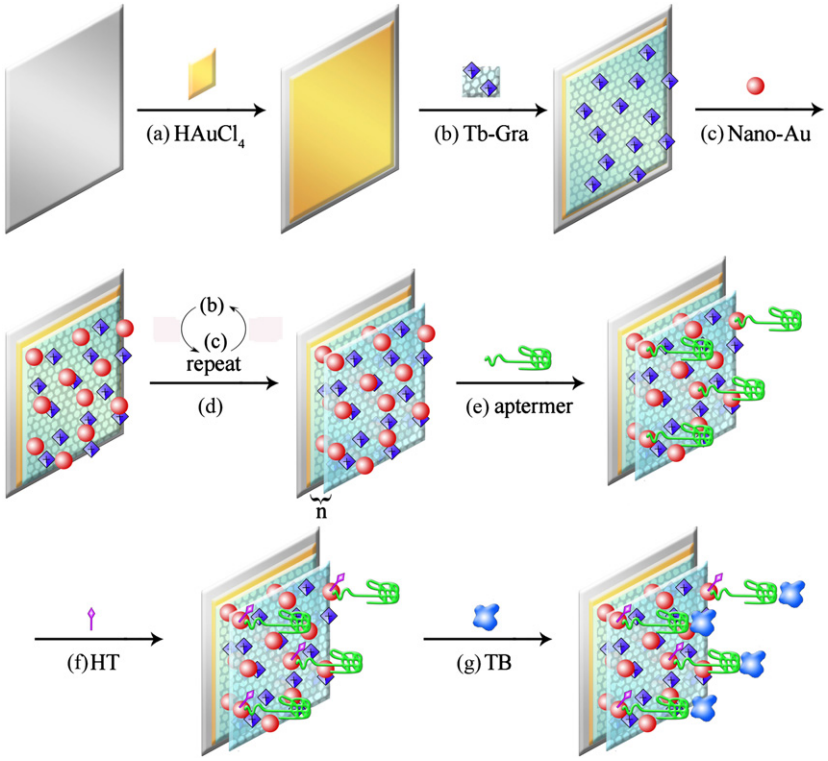

Fig. 1. The schematic illustration of the aptasensor fabrication progress (a) formation of nano-Au film by electrodepositing $HAuCl_4$; (b) positive-charged adsorption of Tb–Gra; (c) negative-charged adsorption of nano-Au (d) repeat step (b) and (c) to form $\{nano\text{-}Au/Gra\}_n$ multilayer films; (e) assembled the thiolated aptamer (f) blocked nonspecific sites with HT; (g) detection of TB.

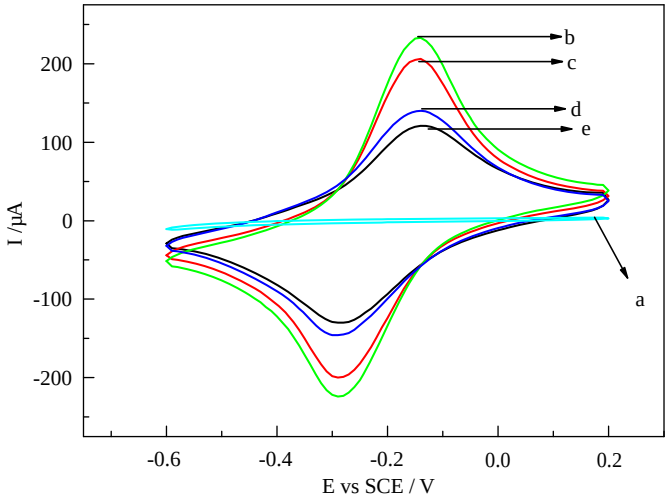

Fig. 2. The CVs of different modified electrodes in 0.1 M PBS containing 0.1 M KCl (pH 7.00): (a) bare glassy carbon electrode electrode; (b) $\{Tb\text{–}Gra/nano\text{-}Au\}_4$ multilayer films modified electrode; (c) combined with TBA; (d) blocked with HT; (e) combined with TB (1 nM). All potentials are given vs. SCE and the scan rate was 100 m V s^{-1}.

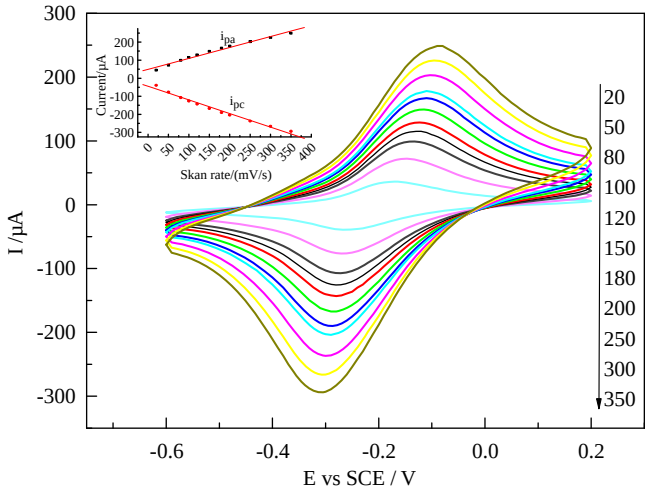

Fig. 3. CVs of the modified aptasesor at different scan rates (from inner to outer):20 m V s^{-1}, 50 m V s^{-1}, 80 m V s^{-1}, 100 m V s^{-1}, 120 m V s^{-1}, 150 m V s^{-1}, 180 m V s^{-1}, 200 m V s^{-1}, 250 m V s^{-1}, 300 m V s^{-1}, 350 m V s^{-1} in 0.1 M PBS containing 0.1 M KCl (pH 7.00) under room temperature. All potentials are given vs. SCE. The insert shows the dependence of redox peak currents on the scan rates.

(Fig. 2a). Owing to the redox probe of Tb–Gra nanocomposites and good conductivity of nano-Au, the multilayer of {Tb–Gra/nano-Au}$_4$ showed a large peak current (Fig. 2b). After assembling TBA, the response was reduced obviously due to the decreased electron transfer capability of the modified electrode (Fig. 2c). Subsequently, the modified electrode was treated with HT, the nonspecifically adsorbed aptamer was removed from the surface and only one end of the aptamer was bound to the surface with all the relevant bases freely available for reaction with TB [38–39]. Such conformation along with the less densely packed monolayer of HT could account for the decrease of peak current (Fig. 2d). After incubating with TB, the steric hindrance was further increased, resulting in a further decrease in current (Fig. 2e). The CVs of the resulting aptasensor at different scan rates were also studied (Fig. 3). The redox peak currents were proportional to the square of scan rates in the range of 20–350 m V s^{-1}, indicating diffusion controlled redox process. Moreover, AFM was

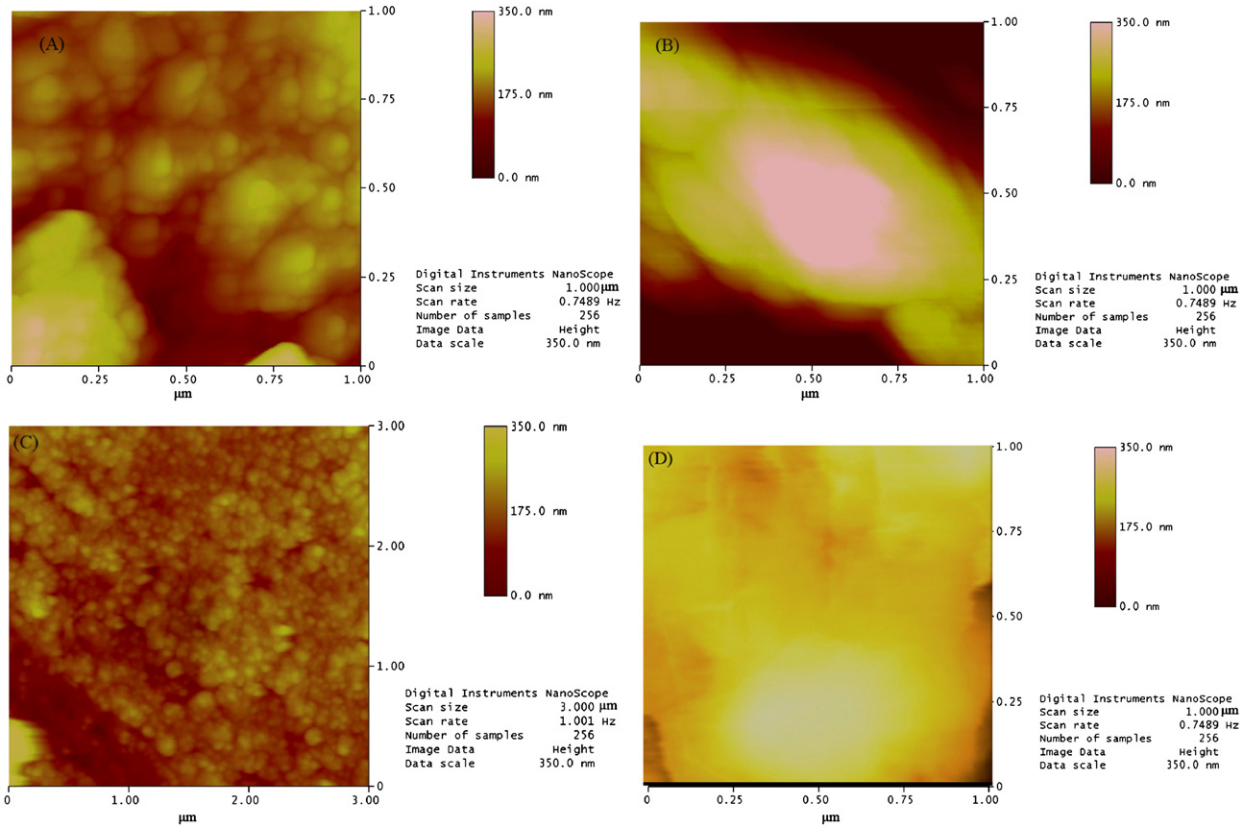

Fig. 4. AFM images: (A) the nano-Au film deposited on the glassy carbon electrode electrode; (B) coating the first layer of Tb–Gra; (C) adsorption of nano-Au (16 nm). (D) coating the second layer of Tb–Gra.

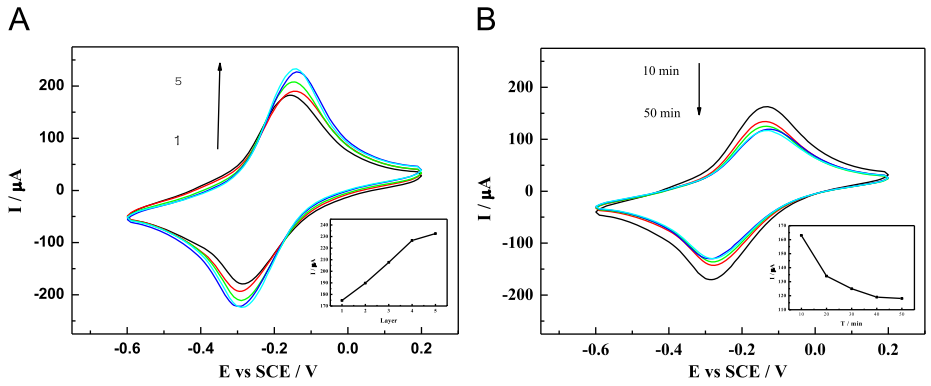

Fig. 5. The optimization of experimental parameter: (A) the optimization of $\{Tb–Gra/nano-Au\}_n$ multilayer. The insert shows the dependence of peak currents on each layernumbers; (B) influence of the incubation time on the current response of the aptasensor. The insert shows the dependence of peak currents on each incubation time.

performed to characterize the morphology of the $\{Tb–Gra/nano-Au\}_n$ multilayer. Fig. 4 exhibited AFM images of the first cycle of the LBL structure modification process. By LBL assembling, the multilayer showed a significant change of the surface morphology. The deposition of $HAuCl_4$ on the electrode surface showed uneven structure with irregular size (Fig. 4A). After Tb–Gra nanocomposites was modified, the surface morphology changed into uniformly distributed (Fig. 4B). When gold nanoparticles were adsorpted, the surface morphology further changed into spherical particles (Fig. 4C). Then another layer of Tb–Gra nanocomposites were dipped on the modified electrode, the surface morphology changed into uniformly distributed again (Fig. 4D). This indicated that the LBL technique could be successfully performed.

3.2. Optimization of experimental conditions for aptasensor

As shown in Fig. 5A owing to the excellent electrochemical activity of Tb–Gra and the good conductivity of nano-Au, the current responses increased with the increasing number of the Tb–Gra/nano-Au layers. However, when the layers reached to 4, the current increased slowly, which indicated a saturation state was reached after 4 times of alternate adsorption. Thus, in our work we selected 4 as the number of $\{Tb–Gra/nano-Au\}_n$ layers.

The incubation time of the TBA modified electrode in TB solution is an important parameter for TB reaction. In the incubation solution of TB (1 nM), the current response decreased rapidly with the increase of incubation time and almost leveled off after 40 min (Fig. 5B). It meant that the building of TBA–TB

complex reached to saturation. Therefore, 40 min of incubation time was used for the detection of TB.

3.3. CV response and calibration curves

In the experiments, under the optimal conditions, the aptasensor was incubated in TB solutions with different concentrations. Fig. 6 shows the calibration curves corresponding to the CV detection of thrombin in the PBS (pH 7.0) containing 0.1 M KCl based on the changes of current intensity (ΔI). There was a linear relationship between ΔI and logarithm of thrombin concentration from 0.001 nM to 80 nM. The linear equation was $\Delta I\,(\mu A) = 0.0439\ \mathrm{Log}\ C_{TB}\ (\mathrm{nM}) + 0.1382$ with a correlation coefficient of 0.9949 and an evaluated detection limit of 0.33 pM. In addition, the analytical performance of the developed aptasensor for thrombin detection was compared with those of other similar Lable-free aptasensors reported in the literatures [6,40–45]. The results were summarized in Table 1. It can be seen that the linear range and detection limit of the proposed aptasensor was greatly improved and a lower detection limit was achieved. The reason for that might be the LBL multilayers can bring in not only more probes to produce an amplified signal, but also more molecular recognition elements to decrease the detection limit.

3.4. Selectivity, reproducibility and stability of the aptasensor

The specificity of the aptasensor played an important role in analyzing biological samples in situ without separation. So the specific recognition to thrombin of the aptasensor has been investigated. Since BSA is an inert protein, whose property is similar to the inert protein in human serum, the selection of BSA as interferent could show the influence of inert protein in assay. HB is a typical active blood protein, so HB as interferent could exhibit the influence of active protein in blood. L-cysteine was chosen as an impurity interferent. Therefore the interferences of BSA, Hb and L-cysteine were investigated to indicate the specificity of the proposed aptasesor.

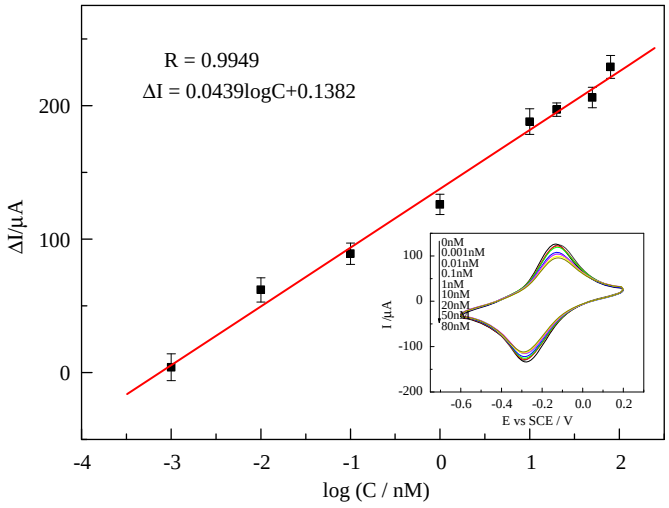

Fig. 6. Calibration curves of the cathodic peak current changes of the aptasensor vs. the TB concentrations range from 0.001 nM to 80 nM under the optimized conditions, which based on the changes of the current response (ΔI). The insert shows CVs of the aptasensor after incubation with each concentration of TB.

In order to test the specificity of this sensing strategy, we used 100 nM of BSA, 100 nM of L-cysteine and 100 nM of HB, respectively to replace 1 nM TB in the same experimental conditions. Different current response signals were obtained. From Fig. 7A we could see that no remarkable change of current was observed in comparison with the result obtained in the presence of thrombin, it was testified that these three interferents could not interact with the TBA. Moreover, the cross-sensitivity of the aptasensor in a mixture of four different substance containing TB was also examined. Even though much higher concentration of BSA (100 nM), Hb (100 nM) and L-cysteine (100 nM) were coexisted in detecting 1 nM of thrombin, The ΔI obtained from the response of complex was almost the same as the ΔI obtained from only TB, which obviously indicated that the BSA, HB and L-cysteine had almost negligible influence for TB detection.

The reproducibility of the proposed aptasensor was investigated at the thrombin concentration of 1 nM by intra- and inter-assay coefficients of variation. The same electrode prepared at five times exhibited similar electrochemical response and the coefficient of variation was 4.2%; five different electrodes in the same batch exhibited good fabrication reproducibility and the coefficient of variation was 5.3%. This demonstrated that the reproducibility of the proposed aptasensor for thrombin detection was acceptable.

In this work, the stability of the LBL multilayer was also investigated. The stability of the successive assays was studied by 100 cycles CV measurements in PBS after being incubated in 1 nM TB. The result suggested that peak currents decreased 3.7% (Fig. 7B). The long-time stability of the aptasensor was investigated in 25-day period. The aptasensor was stored in the refrigerator at 4° C and measured every 5 day. During the first 5 day, the response current decreased by about 0.8% of its initial response, in the next 10 day it decreased by about 6.8%, and over 25 day, the peak current decreased 9.4%.This indicated that the developed aptasensor had a sufficient stability. Obviously, the assembled aptasensor achieved sufficient stability for detection of thrombin.

3.5. Analytical application of the aptasensor

The assay of the target analytes in a series of real samples was investigated by detecting TB in human serum sample. The standard addition method was employed to evaluate the applicability of the proposed aptasensor. Herein, a series of samples

Table 1
Performance compared with other similar lable-free aptasensors for thrombin detection.

Detection technology	Redox probe	Linear range (nM)	Detectin limit	Reference
CVs	Nickel hexacyanoferrates nanoparticles	0.01–50	6.3 pM	[40]
QCM	Methylene blue	10–100	3 nM	[41]
EIS	$[Fe(CN)_6]^{3-/4-}$	0.12–50	40 pM	[42]
DPV	Ferrocene	0.001–50	0.5 pM	[43]
DPV	Thionine	0.05–40	3 pM	[44]
EIS	Polyamidoamine dendrimer	1–50	10 pM	[45]
CVs	Methylene blue	0.12–46	40 pM	[6]
CVs	Toluidine blue-graphene nanoparticles	0.001–80	0.33 pM	This work

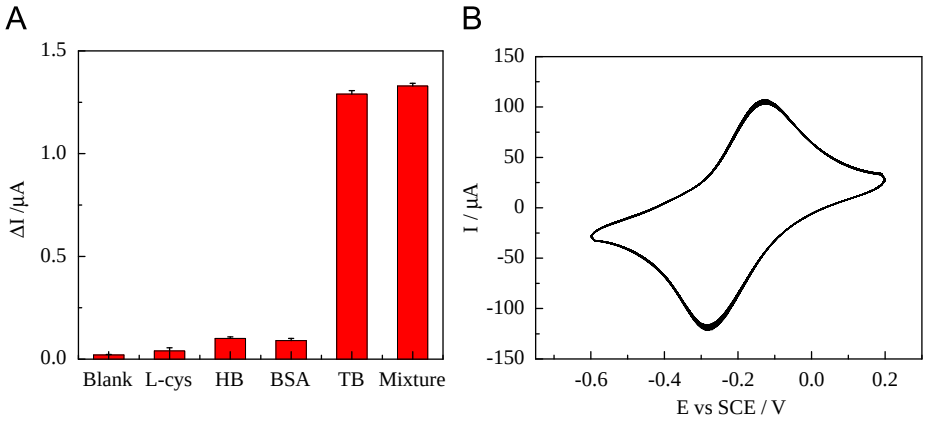

Fig. 7. (A) Comparison of the ΔI of the peaks currents by employing different interferent: [TB]=1 nM; [Hb], [BSA], [L-cys]=100 nM. The mixture was consisting of TB, Hb, BSA, L-cysteine. All curves were registered in 0.1 M PBS containing 0.1 M KCl (pH7.00). Potential scan rate was 100 m V s^{-1}. (B) 100 cycles CV measurements in PBS containing 10 mM KCl (pH 7.00) after being incubated in 1 nM TB.

Table 2
Determination of thrombin added in human blood serum ($n=3$) with the proposed aptasensor.

Sample	Standard value/μA (I_0)	Value/μA (I)	Recovery (I/I_0) (%)	RSD (%)
1	−128.4	−134.8	105	5.9
2	−125.7	−127.1	101	4.5
3	−122.0	−126.9	103	2.4
4	−115.8	−116.9	101	5.7
5	−114.9	−110.3	96	4.3
6	−114.0	−107.2	94	3.1

were prepared by adding TB of different concentrations to human blood serum (obtained from the Ninth People's Hospital of Chongqing, China). The analytical results for TB were shown in Table 2. From Table 2, we could see that the recovery (between 94% and 105%) and relative standard deviation values (between 2.4b% and 5.9%) were acceptable, which clearly indicated the potentiality of this aptasenor for TB detection in real biological samples.

4. Conclusion

In this paper, the prepared Tb–Gra nanocomposites combined the advantages of the graphene (unique electrical, enlarged active surface) and toluidine blue (excellent redox activity) together with nano-Au (good biocompatibility, conductivity and stability). Based on this nanocomposites and nano-Au, a sensitive and lable-free aptasensor for TB was developed, in which the thiolated TBA was directly immobilized on the redox compounds of {Tb–Gra/nano-Au}$_4$ multilayer films modified electrode surface as a protein capture. The prepared aptasensors exhibited high response sensitivity, a low detection limit, and a wide linear range to TB. Besides, compared with the molecular monolayer biosensors, these LBL multilayers bring in more redox probes and more molecular recognition elements which could improve the sensitivity of the biosensor.

Acknowledgements

This work was supported by the National Natural Science Foundation of China (21075100), the Chinese Ministry Foundation for excellent young teachers (2002-40), the Natural Science Foundation of Chongqing City (CSTC-2004BB4149, 2005BB4100), State Key Laboratory of Electroanalytical Chemistry (SKLEAC 2010009) and High Technology project Foundation of Southwest University (XSGX 020) China.

References

[1] M.A. Mir, M. Vreeke, I. Katakis, Electrochem. Commun. 8 (2006) 505.
[2] C. Tuerk, L. Gold, Science 249 (1900) 505.
[3] A.D. Ellington, J.W. Szostak, Nature 346 (1900) 818.
[4] C.L.A. Hamula, J.W. Guthrie, H. Zhang, X.F. Li, X.C. Le, Anal. Chem. 25 (2006) 681.
[5] Y.F. Huang, H.T. Chang, W. Tan, Anal. Chem. 80 (2008) 567.
[6] Y.L. Yuan, R. Yuan, Y.Q. Chai, Y. Zhuo, Z.Y. Liu, Anal. Chim. Acta 668 (2006) 171.
[7] N.A. Hernandez-Rodriguez, E. Correa, A. Contreras-Paredes, Rev. Inst. Nal. Cancerol 43 (1997) 65.
[8] V. Pavlov, Y. Xiao, B. Shlyahovsky, I. Willner, Am. Chem. Soc. 126 (2004) 11768.
[9] X.Y. Wang, J.M. Zhou, W. Yun, S.S. Xiao, Z. Chang, P.G. He, Y.Z. Fang, Anal. Chim. Acta 598 (2007) 242.
[10] K. Lettau, M. Katterle, A. Warsinke, F.W. Scheller, Biosens. Bioelectron. 23 (2008) 1216.
[11] Y.L. Wang, D. Li, W. Ren, Z.J. Liu, S.J. Dong, E. Wang, Chem. Commun. 22 (2008) 2520.
[12] Y. Xiao, A.L. Arica, J.H. Alan, W.P. Kevin, Angew. Chem. Int. Ed. 44 (2005) 5456.
[13] B.L. Li, Y.L. Wang, H. Wei, S.J. Dong, Biosens. Bioelectron. 23 (2008) 965.
[14] P. He, L. Shen, Y. Cao, D. Li, Anal. Chem. 79 (2007) 8024.
[15] X.R. Zhang, B.P. Qi, Y. Li, S.S. Zhang, Biosens. Bioelectron. 25 (2009) 259.
[16] K.S. Novoselov, A.K. Geim, S.V. Morozov, D. Jiang, Y. Zhang, S.V. Dubonos, I.V. Grigorie, A.A. Firsov, Science 306 (2004) 666.
[17] J.S. Wu, W. Pisula, K. Mullen, Chem. Rev. 107 (2007) 718.
[18] J.S. Bunch, A.M. Vander Zande, S.S. Verbridge, I.W. Frank, D.M. Tanenbaum, J.M. Parpia, H.G. Craighead, P.L. McEuen, Science 315 (2007) 490.
[19] M.J. Allen, V.C. Tung, R.B. Kaner, Chem. Rev. 110 (2010) 132.
[20] Y.B. Zhang, Y.W. Tan, H.L. Stormer, P. Kim, Nature 438 (2005) 201.
[21] C.G. Lee, X.D. Wei, J.W. Kysar, J. Hone, Science 321 (2008) 385.
[22] S. Ghosh, I. Calizo, D. Teweldebrhan, E.P. Pokatilov, D.L. Nika, A.A. Balandin, Appl. Phys. Lett. 92 (2008) 151911.
[23] Y.H. Lu, W. Chen, Y.P. Feng, P.M. He, Phys. Chem. 113 (2009) 2.
[24] M.H. Yang, H. Javadi, S.Q. Gong, Biosens. Bioelectron. 26 (2010) 560.
[25] Z.Y. Zhong, D. Wu, D. Wang, J.L. Shan, Y. Qing, Z.M. Zhang, Biosens. Bioelectron. 25 (2010) 2379.
[26] F.Y. Kong, M.T. Xu, J.J. Xu, H.Y. Chen, Talanta 85 (2011) 2620.
[27] S. Stankovich, S. Dikin, D.A. Dommett, G.H.B. Kohlhaas, K.M. Zimney, E.J. Stach, E.A Piner, R.D. Nguyen, S.T. Ruoff, Nature 442 (2006) 282.
[28] H. Shiigi, S. Tokonami, H. Yakabe, T. Nagaoka, J. Am. Chem. Soc. 127 (2005) 3280.
[29] W. Lu, Y. Jin, G. Wang, D. Chen, J. Li, Biosens. Bioelectron. 23 (2008) 1534.
[30] Y. H. Bai, J. Y. Li, J. J. Xu, H. Y. Chen, Analyst. 135 (2010) 1672.
[31] M.V. Melgardt, P.O. Daniel, J.S. Schalk, M.L. Yuri, Adv. Drug Delivery Rev. 63 (2011) 701.
[32] P. Bertrand, A. Jonas, A. Laschewsky, R. Legras, Macromol. Rapid Commun. 21 (2000) 319.
[33] A.L. Becker, A.P.R. Johnston, F. Caruso, Macromol. Biosci. 10 (2010) 488.

[34] A.P.R. Johnston, E.S. Read, F. Caruso, Nano Lett. 5 (2005) 953.
[35] K.F. Ren, J. Ji, J.C. Shen, Biomaterial 27 (2006) 1152.
[36] K.I. Sano, K. Shiba, MRS Bull. 33 (2008) 52.
[37] G. Frens, Nat. Phys. Sci. 241 (1973) 20.
[38] R. Levicky, T.M. Herne, M.J. Tarlov, S.K. Satija, Am. Chem. Soc. 120 (1988) 9787.
[39] A.E. Radi, J.L. Acero Sanchez, E. Baldrich, C.K. OSullivan, Anal. Chem. 77 (2005) 6320.
[40] L.J. Bai, R. Yuan, Y.Q. Chai, Y.L. Yuan, L. Mao, Y. Zhuo, Analyst 136 (2011) 1840.
[41] A. Porfirieva, G. Evtugyn, T. Hianik, Electroanalysis 19 (2007) 1915.
[42] X.X. Li, L.H. Shen, D.D. Zhang, H.L. Qi, Q. Gao, F. Ma, C.X. Zhang, Biosens. Bioelectron. 23 (2008) 1624.
[43] X.R. Liu, Y. Li, J.B. Zheng, J.C. Zhang, Q.L. Sheng, Talanta 81 (2010) 1619.
[44] Y.L. Yuan, R. Yuan, Y.Q. Chai, Y. Zhuo, L.J. Bai, Y.H. Liao, Biosens. Bioelectron. 26 (2010) 881.
[45] Z.X. Zhang, W. Yang, J. Wang, C. Yang, F. Yang, X.R. Yang, Talanta 78 (2009) 1240.